Simulation Calculation and Analysis of Building Energy Consumption of Multi-Story Glued Laminated Timber Structures

Yuying Zou,[a] Xiaoyu Gu,[a] Patrick Adjei,[b] Zheng Wang,[a,*] and Yujie Huang[c]

As the only renewable building material, wood has a strong carbon sequestration effect. Thus, timber structures have the natural advantages of saving energy and reducing emissions. Currently, the research objects of building energy consumption are rarely timber structures. To further control the operational energy consumption of timber structures, this paper takes six-story glued laminated timber beam-column frame and light wood-frame shear wall structures as the research objects. Building energy consumption research is conducted through testing the heat transfer coefficient of the envelope structure, air circulation ratio, and Building Information Modeling (BIM) technology on-site. The results show that the energy consumption of the building is consistent with the current energy consumption of small- and medium-sized office buildings, and the heat gain and loss of the building are mainly due to solar radiation and heat conduction of the envelope, respectively. The airtightness of the building has the greatest influence on the energy consumption of the building, and the type of building structure and window-to-wall ratio have little influence on the energy consumption of the building.

*Contact information: a: College of Materials Science and Technology, Nanjing Forestry University, Nanjing 210037, China; b: College of Civil Engineering, Nanjing Forestry University, Nanjing 210037, China; c: College of Civil Engineering, Southeast University, Nanjing 210037, China; * Corresponding author: wangzheng63258@163.com*

INTRODUCTION

Wood is characterized by its strong carbon fixation capacity and good stiffness (Wang *et al.* 2014, 2015, 2016, 2018, 2019). Therefore, timber structures naturally have the advantages of being low-carbon and environmentally friendly (Lin *et al.* 2015; Zuo and Wang 2017; Geng 2018; Liu *et al.* 2022). However, the operational phase of a building is highly energy-intensive. Glued laminated timber structures are mostly used in public buildings, which have the second highest energy consumption and carbon emissions of all buildings in the operational phase (Leonel *et al.* 2022; Zhang *et al.* 2022a,b). Therefore, studying the operational energy consumption of glued laminated timber structures and its control within a reasonable range can successfully reduce the amount of energy consumption during the whole life cycle.

Building airtightness, as an important influencing factor of energy consumption in the operational phase of buildings, has been studied by many scholars. Many studies abroad have used a probabilistic approach to study architectural physics (Peng *et al.* 2018; Wang

and Roger 2021, 2022). The two main methods for testing building airtightness internationally are the blower door method and the tracer gas method (Xiong *et al.* 2022). Through the use of these two testing methods to test the airtightness and permeability of residential buildings, it was found that factors such as the quality of the building and the sealing of ventilation places such as windows and doors, have a particular influence on the overall building airtightness (Kalamees 2007; Sfakianaki *et al.* 2008; Pan 2010; Ambrose and Syme 2017). Furthermore, by designing a prediction model to test the airtightness of the building, the airtightness in calculation results of energy consumption are reliable, provided that the requirements are met (Alfano *et al.* 2012; Feng *et al.* 2014; Šadauskienė *et al.* 2016). In contrast, fewer studies have been conducted to calculate the effect of building airtightness on energy consumption by building numerical models. In many research studies, numerical simulations have been used to calculate and analyze the energy consumption of residential buildings. The multi-objective optimization algorithm NSGA-II, DeST software, and CFD software have been used. It has been found that airtightness has a negative correlation with energy consumption for buildings (Zhang *et al.* 2016; Ma and Cong 2020; Cao *et al.* 2022; Lin and Song 2022). In heating and cooling, heat transfer and airtightness are important factors affecting energy consumption. Improvement of heat transfer efficiency can reduce energy consumption, while improvement of air tightness can avoid loss of heat or cold air. Therefore, the study and improvement of these two factors are important to increase the efficiency of energy utilization and reduce the cost. In previous studies, there have been many studies on the effects of heat transfer and air tightness on energy consumption. However, most of the studies have been conducted on concrete structures, steel structures, *etc*., and fewer studies have been conducted on wood-framed buildings.

There have been few simulations and studies on the energy consumption of timber structures worldwide and even fewer on public buildings. The boundary conditions for the study of building energy consumption are primarily determined by referring to the standard values defined in each country's relevant standards. However, these standards involve the heat transfer coefficient of the envelope, building airtightness, and building operation time that cannot be quantified accurately. Fewer studies have been conducted on the airtightness aspects of wood-framed buildings, but their impact on building energy consumption has been significant. Therefore, this paper takes a six-story glued laminated timber beam-column frame and light wood-frame shear wall as the research objects. On-site measurements of the heat transfer coefficient of the envelope and air circulation ratio were conducted. Using the measured data and the BIM technology, the annual energy consumption of the building was simulated, the priority of its airtightness influencing factors were explored, and the accuracy of the simulation calculations was improved.

EXPERIMENTAL

Material and Methods

Test subjects

The research object of this paper is the Research and Development (R&D) center building of Shandong Dingchi Wood Industry Co. The building is a six-story glued laminated timber beam-column frame-light wood shear wall system building. Except for the stairwell wall, the rest of the wall is SPF specification lumber composition of the shear wall. The stairwell wall material is made of SPF specification lumber made of cross-

laminated timber (CLT). The beams, columns and floor materials are SPF glued laminated timber with a longitudinal length of 66.9 m, a transverse width of 17.4 m, and a total height of 24.7 m. The floor area is 4778.5 m^2. The number of floors of the main structure of the building is part six and part four, as shown in Fig. 1. The building is located in Penglai City, Shandong Province, which is in a cold region according to Appendix A.0.3 of GB 50176-2016 (2016), as shown in Fig. 2. The detailed structural drawings of each part of the building are shown in Fig. 3.

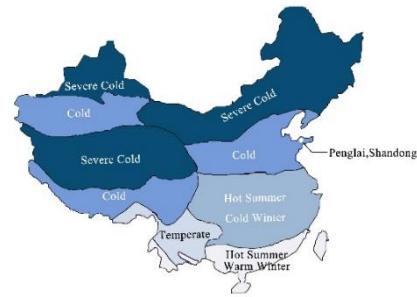**Fig. 1.** R & D center building exterior rendering

Fig. 2. Building location schematic

a. Details of light wood frame exterior wall

b. Details of light wood frame interior wall

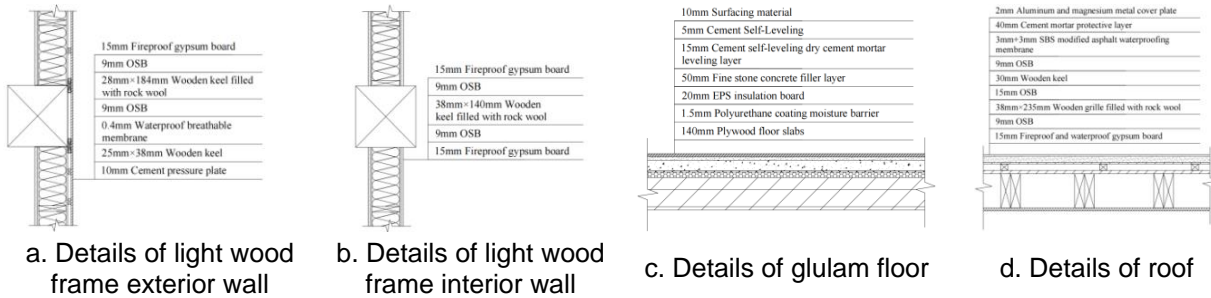c. Details of glulam floor

d. Details of roof

Fig. 3. Details of the R&D center building

Because the heat transfer coefficient test needs to arrange sensors, and according to the requirements in JGJ/T 357-2015 (2015), the measured area should not be less than 1.2 m × 1.2 m to meet the test requirements and facilitate the test. The office on the south side of the first floor is selected as the test space, as shown in Fig. 4. A diagonal line indicates the tested wall in the right figure. The internal material parameters of each structure are shown in Table 1.
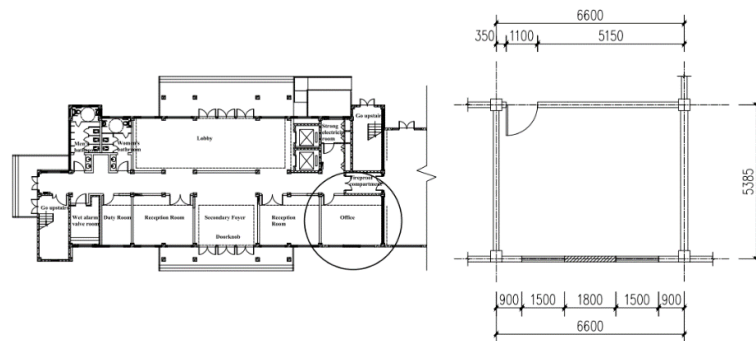

**Fig. 4.** Schematic diagram of heat transfer coefficient test area

Table 1. Material Parameter Table of Wall, Floor, and Roof of R&D Center Building

Material Name	Density ρ (kg/m³)	Specific Heat Capacity C (J/(kg·K))	Thermal Conductivity λ (W/(m·K))
Fireproof gypsum board	1050	1050	0.330
Oriented strand board	593	1400	0.340
SPF wall studs	500	2510	0.140
Rockwool	100	1220	0.041
Waterproof breathable membrane	1100	1000	1.000
Wooden keel	500	2510	0.140
Cement pressure plate	350	1300	0.082
SPF glued laminated timber	600	2510	0.170
EPS insulation board	25	1400	0.035
Fine stone concrete	2100	920	1.280
Cement mortar	1800	1050	0.930
Magnesium and aluminum metal plate	2750	899	229
Waterproof asphalt membrane	600	1470	0.17

Test Equipment and Methods

Wall heat transfer coefficient testing equipment and method

The test instruments in this study are mainly an HT-1 field heat transfer coefficient tester, heat flow meter sensor, and Pt1000 temperature sensor from Beijing Borin Jiji Technology Co. Based on the heat flow meter method, regarding GB/T 34342-2017 (2017), JGJ/T 357-2015 (2015), and GB/T 23483-2009 (2009). The schematic layout of measurement points is shown in Fig. 5, and the test site is shown in Fig. 6.
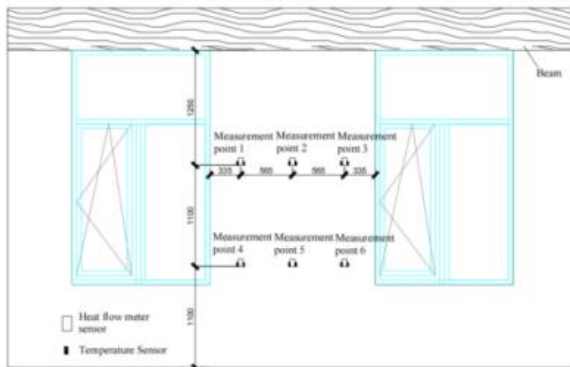
**Fig. 5.** Schematic diagram of sensor positioning   **Fig. 6.** Sensor layout on site

Building airtightness testing equipment and methods

This test was performed using the fan pressure method as specified in GB/T 34010-2017 (2017). The test methods are mainly divided into two categories: the decompression method and the pressurization method. The test results obtained by the decompression method are generally slightly larger than those by the pressurization method. The higher the airtightness of the building, the smaller the difference between the results measured by the two methods.

Table 2. Building Airtightness Testing Equipment

| Instrument Name	Model	Test Range	Precision	Quantity
Blower door test system	TEC DG1000	-2500 to 2500 Pa	0.12Pa	1
Infrared thermal imaging camera	Testo872	-30 to +100 °C	0.06 °C	1
Environmental temperature and humidity detector	JT2020-9	-20 to 60 °C/0 to 95%RH	0.1 °C /0.1%	1
Empty box air pressure gauge	DYM3	800 to 1064 hPa	2 hPa	1
Pressure, velocity, and volume meter	TSI-5825	0 to 3725 Pa	1.5%	1
Infrared rangefinder	SW-M60A	0 to 60 m	2%	1

When testing, all the external doors and windows of the tested space should be closed, and all the internal doors should be opened so that the pressure in the test space can be guaranteed to be relatively uniform. The excess holes in the air conditioner or walls should be sealed with suitable materials to prevent errors in the test results, as shown in Fig. 7. When measuring, the first step is to measure the net volume of the space to be measured, the indoor and outdoor temperature and humidity and the atmospheric pressure. According to the target pressure, the pressure inside the room is pressurized or depressurized. After the indoor pressure is relatively stable, the indoor pressure will be collected several times. The air leakage volume can be calculated based on the atmospheric pressure, indoor and outdoor temperature, humidity, and pressure difference. The number of air changes of the test object is obtained from the air leakage volume and the net volume of the room. The test schematic and the device diagram are shown in Fig. 8 and Fig. 9, respectively.

a. Window blocking   b. Ceiling blocking   c. Vent blocking   d. Corner blocking
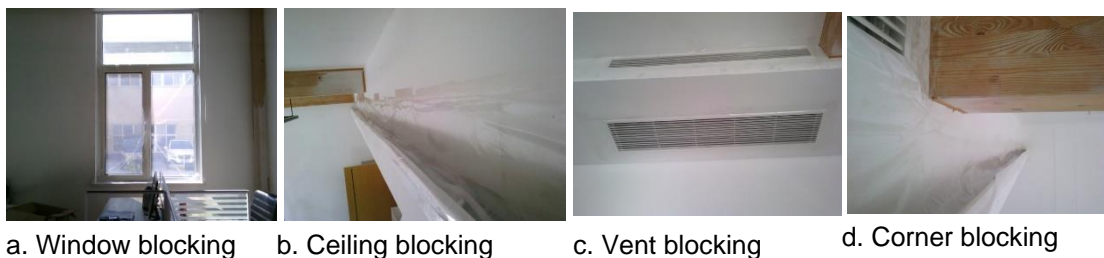
Fig. 7. Indoor hole blocking
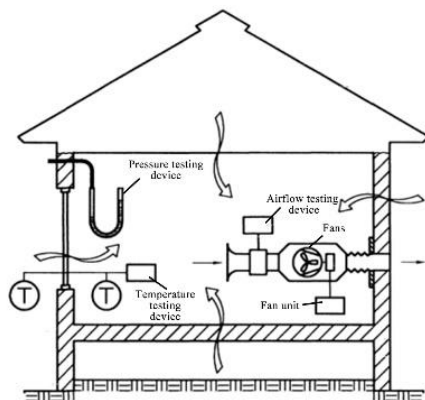
Fig. 8. Schematic diagram of the building test system
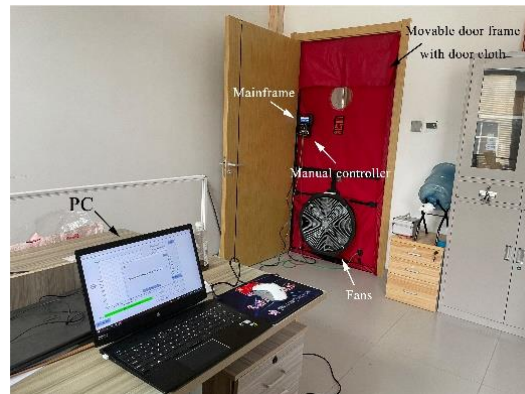
Fig. 9. Installation and connection of blower door

The test equipment is located inside the building, so the wind speed outside the test space is 0 m/s. The indoor temperature is 26.8 °C, the outdoor temperature is 19.1 °C, and the atmospheric pressure is 1.025×105 Pa.

Modeling and parameter setting for building energy simulation calculation

In this paper, Revit software developed by Autodesk was used to establish a 3D parametric model and simulate the building energy consumption through Ecotect Analysis 2010, as shown in Fig. 10.

a. Parametric 3D model

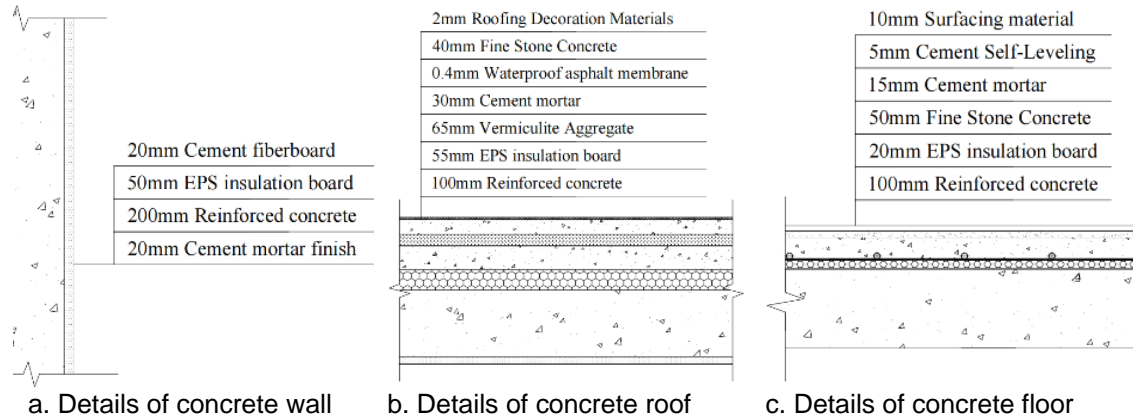b. Building energy consumption calculation model
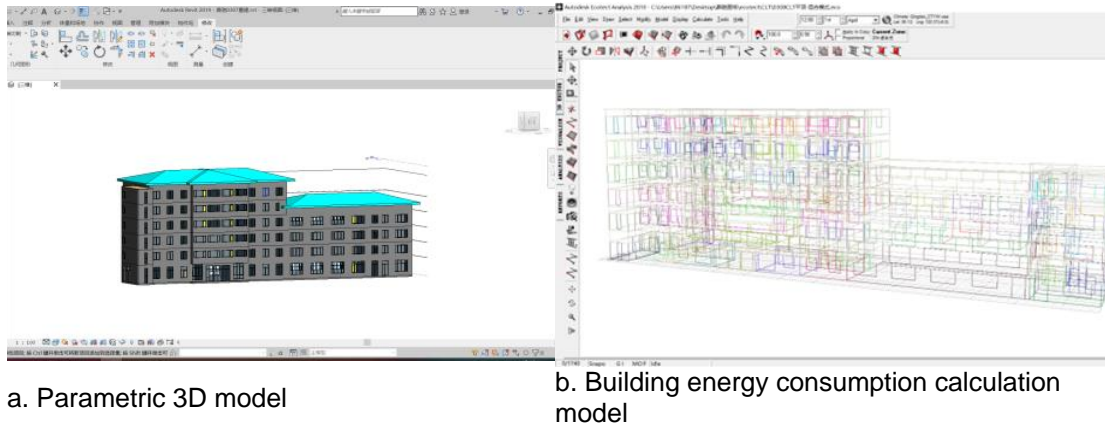
Fig. 10. Building simulation models

To study the influence of different structural types on the energy consumption of the building, the main structure was designed as a concrete structure and CLT structure, respectively, while keeping the floor plan and facade of the building unchanged to compare the change of energy consumption of the building. The structural outline of the existing building is shown in Fig. 4. The internal material parameters of each structural elements are shown in Table 1. The CLT and concrete structure wall, roof, and floor slab samples are shown in Figs. 11 and 12, respectively, and the internal material parameters are shown in Table 3 (Dong *et al.* 2019).

a. Details of CLT wall   b. Details of CLT roof   c. Details of CLT floor
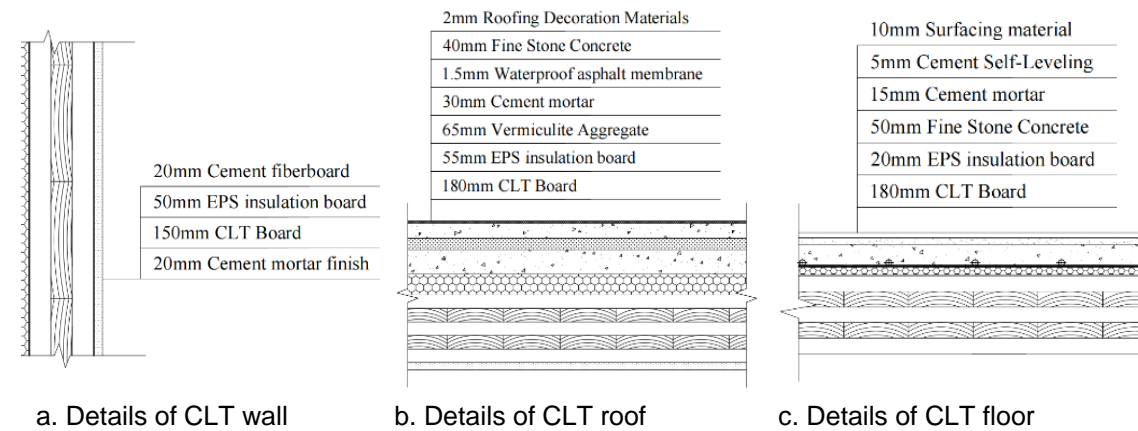
Fig. 11. CLT structural component details

a. Details of concrete wall   b. Details of concrete roof   c. Details of concrete floor

Fig. 12. Details of concrete structural components

Table 3. CLT and Concrete Structure Exterior Wall, Floor, and Roof Material Parameter Table

Materials	Density ρ (kg/m³)	Specific Heat Capacity C (J/(kg·K))	Thermal Conductivity λ (W/(m·K))
Cement fiberboard	350	1300	0.082
CLT	500	1500	0.130
Cement self-leveling	1800	1050	0.930
Surfacing material	240	732	0.055
Vermiculite aggregate	450	837	0.450
Concrete blocks	2300	1000	1.630
Reinforced concrete	2000	1050	2.300

This study simulates a full year of work time *versus* rest time and the enterprise adopts the model of a single break with regular rest on legal holidays, including 79 days of holidays and 286 days of working days.

Referring to GB55015-2021 (2021), the boundary conditions of each room are set differently according to the personnel density, working status, and lighting in different areas (Table 4). The presence of room personnel in the room at each time of the same day is shown in Table 5.

Table 4. Simulation Parameters of Internal Gains

Room Category	Number of People	Area Per Capita (m²)	Illumination Standard Value (lx)	Lighting Power Density (W/m²)	Electrical Power Density (W/m²)	Dress (clo)	Air Conditioning
Manager's office	1	-	300	8	10	1	Yes
Small office	4	-	300	8	15	1	Yes
Medium/Large office	-	4.5	300	8	15	1	Yes
Meeting room	-	5-10	500	8	10	1	Yes
Restrooms	-	-	100	4	0	1	No
Aisle	-	0	50	4	0	1	No
Stairwell	-	0	50	2	0	1	No

Table 5. Hourly Rate of Room Personnel

Time	1	2	3	4	5	6	7	8	9	10	11	12
Proportion (%)	0	0	0	0	0	0	0	10	50	95	95	80
Time	13	14	15	16	17	18	19	20	21	22	23	24
Proportion (%)	80	95	95	95	30	30	0	0	0	0	0	0

The standard value of illumination range of 50 to 500 lx, the lighting power density of 2 to 8 W/m^2, and holiday time were set to the off state according to the various space and office staff work requirements. Lighting usage at various times during the working day on the same day, was as shown in Table 6.

Table 6. Lighting Usage Time

Time	1	2	3	4	5	6	7	8	9	10	11	12
Proportion (%)	0	0	0	0	0	0	0	10	50	95	95	80
Time	13	14	15	16	17	18	19	20	21	22	23	24
Proportion (%)	80	95	95	95	30	30	0	0	0	0	0	0

The indoor temperature was limited to 20 to 26 °C. When the temperature was below or above this range, the air conditioner would automatically start working for cooling or heating to ensure the comfort of the indoor staff. The air conditioner was set to be off during the holidays. Air conditioning is used during the hours shown in Table 7, and not during the hours not shown in the table.

Table 7. Air Conditioner Usage Time

Room Category	Opening time	Cooling Temperature (℃)	Heating Temperature (℃)
Manager's office	8:00 to 17:00	26	20
Small office	8:00 to 17:00	26	20
Medium/Large office	8:00 to 17:00	26	20
Meeting room	9:00 to 10:00	26	20

The power density of electrical appliances was 10 to 15 W/m^2, and the lighting was turned off during holidays. According to different spaces and the operational needs of office workers, the usage of the appliance at various times during the 24-h period on the same working day is shown in Table 8.

Table 8. Use Time of Electrical Appliances

Time	1	2	3	4	5	6	7	8	9	10	11	12
Proportion (%)	0	0	0	0	0	0	0	10	50	95	95	50
Time	13	14	15	16	17	18	19	20	21	22	23	24
Proportion (%)	50	95	95	95	30	30	0	0	0	0	0	0

When the number of air changes increased from 0.5 to 5 h^{-1}, respectively, the change in building energy consumption was calculated again using 0.5 as the step length to investigate the impact of airtightness on building energy consumption.

This simulation used the Chinese meteorological database dedicated to Ecotect Analysis software. Because the data of Penglai city is not available in the database, the data of Qingdao city, which is the nearest typical meteorological year to Penglai city, was used as a substitute in the calculation.

RESULTS AND ANALYSIS

Wall Heat Transfer Coefficient Test

According to section 3.4 of GB 50176-2016 (2016), the thermal resistance R of a single homogeneous material is given as Eq. 1,

$$R = \delta/\lambda \tag{1}$$

where R is the thermal resistance of the material layer (m^2·K/W), δ is the thickness of the material layer (m), and λ is the thermal conductivity of the material (W/(m·K)).

The heat transfer resistance R_0 for heat transfer from the flat wall of the enclosure is given as Eq. 2,

$$R_0 = R_i + \sum R + R_e \tag{2}$$

where R_0 is the thermal resistance of the flat wall of the enclosure (m^2·K/W), $\sum R$ is the total thermal resistance of the internal layers of the enclosure (m^2·K/W), R_i is the heat transfer resistance of the internal surface (m^2·K/W), and R_e is the heat transfer resistance of the external surface (m^2·K/W).

The heat transfer coefficient K of the flat wall of the enclosure structure is given as Eq. 3,

$$K = 1/R_0 \tag{3}$$

where in Eq. 3 K is the enclosure structure flat wall heat transfer coefficient (W/(m^2·K)).

Because the shear wall of light wood frame structure is constructed as a hollow wall, the insulation material is placed inside the wall, and the stud is in the same plane, so the heat transfer coefficient is inconsistent within each area of the wall. For this reason, the heat transfer coefficient of the wall, K, is taken as the weighted average of the percentage of the projected area and the heat transfer coefficient in the area of the studs and the percentage of the projected area and the heat transfer coefficient in the area of the insulation wool, *i.e.* (Dong and Li 2018) Eq. 4,

$$K = S_S K_S + S_I K_I \tag{4}$$

where K is the light wood structure shear wall average heat transfer coefficient (W/(m^2·K)), S_S is the stud area percentage of projected (%), K_S is the stud area average heat transfer coefficient (W/(m^2·K)), S_I is the insulation wool area projection area percentage (%), and K_I is the insulation wool area average heat transfer coefficient (W/(m^2·K)).

From the data in Table 1, it is calculated that: $K_S = 0.732[\text{W} / (\text{m}^2 \cdot \text{K})]$, $K_I = 0.354[\text{W} / (\text{m}^2 \cdot \text{K})]$, $S_S = 12.7\%$, and $S_I = 87.3\%$. It follows theoretically that:

$$K_{\text{Theory}} = S_S K_S + S_I K_I = 0.402[\text{W} / (\text{m}^2 \cdot \text{K})] \tag{5}$$

Taking measurement point 1 as an example, the temperature and heat flow curves are shown in Fig. 13. On 10.19, the outdoor temperature increased, so additional heating measures were taken indoors to ensure the temperature difference between the inside and outside surfaces of the walls.
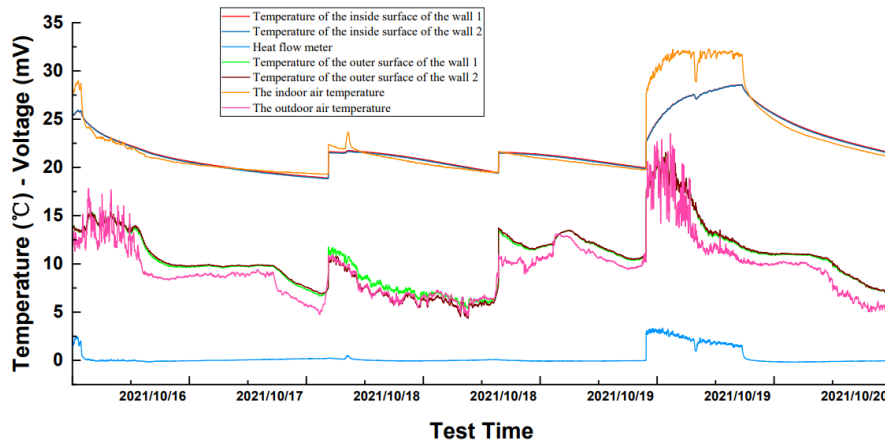

Fig. 13. Heat transfer coefficient test value curve of envelope

The comparison between the test results of the heat transfer coefficient of the wall and the theoretical values are shown in Table 9.

Table 9. Comparison of Field Test Value and Theoretical Value of Heat Transfer Coefficient

Test Points	Test Value [W/(m^2·K)]	Theoretical Value [W/(m^2·K)]	Relative Error (%)
1	0.329		-7.06
2	0.340		-3.95
3	0.379		7.06
4	0.347	0.354	-1.98
5	0.387		9.32
6	0.332		-6.21
Average value	0.351		-0.847

The difference between the average value of the wall heat transfer coefficient test and the theoretical value was only 0.847%, which demonstrates that the test was accurate and the theoretical value was the same as the actual situation. Therefore, the wall meets the design requirements for the thermal performance of walls in cold regions of China, and the theoretical value can be substituted into the building energy simulation software to simulate the annual energy consumption of the building.

Building Airtightness Testing

The airtightness test results of the first-floor office in the entirely blocked state are plotted as a function, as shown in Fig. 14, and the related test results are shown in Table 10.
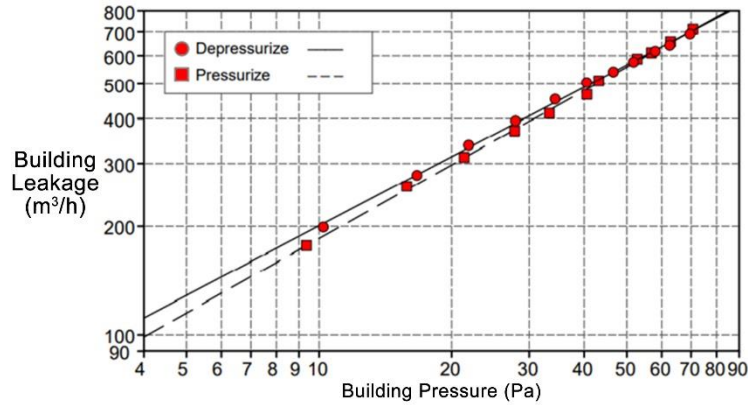
Fig. 14. Airtightness test function diagram of the first-floor office completely blocked state

Table 10. Test Results of the Complete Airtightness of the Office on the First Floor

| Test Category	Air Leakage q50 (m³/h)	Number of Air Changes n_{50} (1/h)	Leakage Area A50 (m²)
Decompression method	565	4.67	0.0172
Pressurization method	557	4.60	0.0170
Average value	564	4.64	0.0171

After sealing the doors and windows with the extra holes, the air change number n_{50} of the office on the first floor was 4.64 h^{-1}, and the airtightness index was in line with the airtightness condition of the normal building. As shown in Fig. 17, the function images obtained by the pressurization method and the depressurization method form a linear relationship, and r^2 was infinitely close to 1. Therefore, the results of this test were deemed reliable. The air leakage and the number of air changes measured by the depressurization method were slightly larger than those by the pressurization method due to the sealing method. In the pressurized mode, the indoor air pressure is greater than the outdoor air pressure, resulting in a pressure difference that causes the air to move from the inside to the outside. The plastic film and tape are squeezed from inside to outside under pressure, making them stick to the wall surface better and seal the hole sufficiently to stop the air from spilling out of the hole. When the decompression method is used, the air rushes into the room from the outside because the interior air pressure is lower than the external air pressure. This forces the plastic film and broad tape away from the wall, resulting in a weaker sealing effect in some areas. This suggests that the sealing effect is weaker than the pressurization method. Therefore, the number of air changes measured by the decompression method is greater than that of the pressurization method, which is also consistent with the regularity specified in the test specification. As a result, the airflow rate of the decompression method is greater than that of the pressurization method.

Simulation of the Building's Annual Operating Energy Consumption

Simulation of the building's annual operating energy consumption

The energy consumption of the R&D center building for cooling and heating in 2022 is shown in Fig. 15. The average energy consumption per unit area of small and medium-sized office buildings in China ranges from 60 to 90 kW·h/(m²·a), and the average energy consumption per unit area of heating and cooling in the R&D center building was

62.7 kW·h/m², which is in line with the normal situation. The energy consumption for cooling is mainly concentrated in summer, *i.e.*, from June to September, with the highest energy consumption in August, while the rest of the months are for heating, mainly in winter and early spring, with the highest energy consumption for heating in January. Shandong province is located in a cold region, and the number of days for heating exceeds the number of days for cooling, and the energy consumption for heating is about 2.5 times that for cooling, which is much larger than that for cooling.
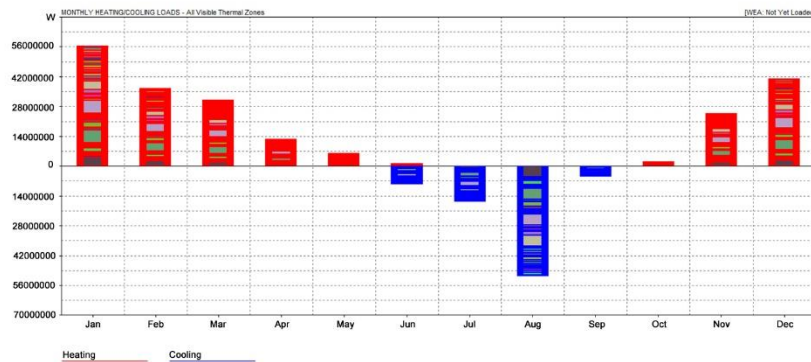
Fig. 15. Histogram of annual cooling and heating energy consumption of R&D center building

The highest energy consumption for heating was 72.2 kW at 10 a.m. on February 19, and the highest energy consumption for cooling was 172.3 kW at 12 p.m. on August 21. Although the coldest temperature of the year occurred on February 22, the difference between the amount of indoor heat transferred to the outside through heat conduction of the envelope and air leakage was not significant compared to February 19. Because the solar radiation was larger during the day on February 22, some of the heat is transferred to the interior through thermal radiation, thus the heating energy consumption is reduced. The year's highest temperature occurred on August 21, which is consistent with the energy consumption for heating and cooling.

The heat gain and loss of this R&D center building throughout the year are shown in Fig. 16.
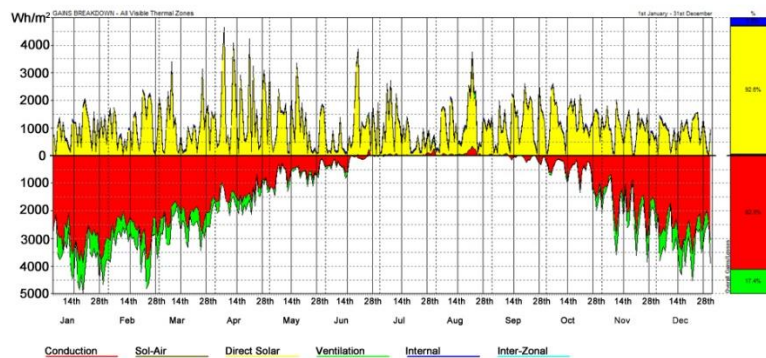
Fig. 16. The annual heat gain and loss curve of the R&D center building

On the one hand, its heat gain relies mainly on solar radiation, accounting for 92.6%. On the other hand, its internal heat production by personnel and electrical equipment, accounting for 5.6%, occurs throughout the year. The rest of the heat gain is air heating, envelope heat transfer, and air inflow, which occurs mainly in summer, *i.e.*, from July to September. The heat loss is mainly due to heat conduction from the envelope, and air leakage, which account for 82.5% and 17.4%, respectively. The heat gain and loss of the building are consistent with the cooling and heating energy consumption, indicating that the simulation fits the actual situation and can import data from the weather forecast to predict the future energy consumption of the building while keeping the rest of the situation unchanged.

Heat gain and loss due to heat conduction of the envelope are always present, reaching the peak of heat loss in winter each year; it starts to turn to heat gain in the summer, but its heat gain is minimal. The trend of heat gain and loss due to air leakage is similar to that of heat conduction. The heat gain due to solar radiation is always present, and the curve is jagged, with great fluctuations in heat gain and no obvious peak pattern. When there are too many clouds in the sky, the amount of solar radiation will be reduced when the sun is blocked. In contrast, it also indicates that the thermal insulation performance of the current building envelope needs to be further optimized, such as increasing the wall thickness, choosing better insulation materials for filling, changing the roof laying materials, and setting up greenery around the building. These are done to ensure greater insulation from solar radiation in summer and reduce heat loss from heat conduction in winter.

Impact of building airtightness on energy consumption

Building airtightness refers to the amount of air infiltration between the outside and inside of a building. To study the influence of building airtightness on building energy consumption throughout the year, the trend of heating energy consumption and cooling energy consumption of the building when the number of air changes was from 0.5 to 5 is calculated separately, using 0.5 as the step length. As shown in Fig. 17, the impact of airtightness on building energy consumption was obvious. In January, for example, for every $0.5\ h^{-1}$ reduction in the number of air changes, heating energy consumption decreased approximately 3,000 kW·h. When the number of air changes in a building decreased from the previous test value to $0.5\ h^{-1}$, annual heating energy consumption decreased approximately 43.5% and cooling energy consumption decreased 9.5%. This shows that increasing the building's airtightness has a significant effect on lowering energy consumption.

Building airtightness affects both heating and cooling energy consumption in buildings, but to different degrees. Building airtightness has a greater impact on heating energy consumption, mainly because heat loss from a building is mainly through air-permeable parts such as walls and windows. If the building is not airtight, indoor heat is easily lost through the breathable parts, resulting in the heating system needing to consume more energy to maintain the indoor temperature. On the contrary, the energy consumption of the cooling system is mainly used to exhaust the indoor heat out, rather than preventing the outdoor heat from entering the room. Therefore, building airtightness has a greater impact on a building's heating energy consumption than cooling. In addition, as the number of air changes decreases, the difference in energy consumption between months gradually decreases. Reducing the number of indoor air changes and improving the airtightness of the building envelope has an obvious effect on the insulation of the indoor environment.

The slope of the energy consumption change curve for cooling in the state of low air exchange number is larger than that in the state of high air exchange number. This is because the amount of indoor heat carried out to the outdoors by the air in summer becomes less and more heat is gathered indoors due to the low air exchange number. However, from the overall energy consumption values, lowering the number of air changes is still beneficial to reducing building energy consumption.

In addition to this, the air leakage rate of a building also affects its airtightness. ISO 9972 (2015) proposes a specific leakage rate using the envelope area and floor area for a reference pressure difference. Hong and Kim (2022) found that for a 2020 building, the leakage rate due to walls is 0.4 for pressurization and 0.5 for depressurization, and the leakage rate due to floor slabs is 0.02 for pressurization and 0.02 for depressurization. The air leakage in the building is mainly in the wall part, as the walls need to be fitted with windows and doors, and the crack area increases with the increase of window and door area.

In this paper, the test object was assembled timber structures, in which ELAE50, which indicates the degree of leakage in the wall area, was 0.0021 m^2/m^2 and 0.0020 m^2/m^2 under pressurization and depressurization and ELAF50, which indicates the degree of leakage in the floor area, was 0.0052 m^2/m^2 and 0.0051 m^2/m^2 under pressurization and depressurization, respectively, both of which were 2.5 times of the degree of leakage in the wall area. The leakage level in the area of the wall was 2.5 times of the leakage level in the area of the floor. This is because the wall and floor laps are prone to gaps, and the gaps are much larger than the cracks at windows and doors, which shows that the areas to be paid attention to in the airtightness design of timber structures are different from those of concrete buildings.
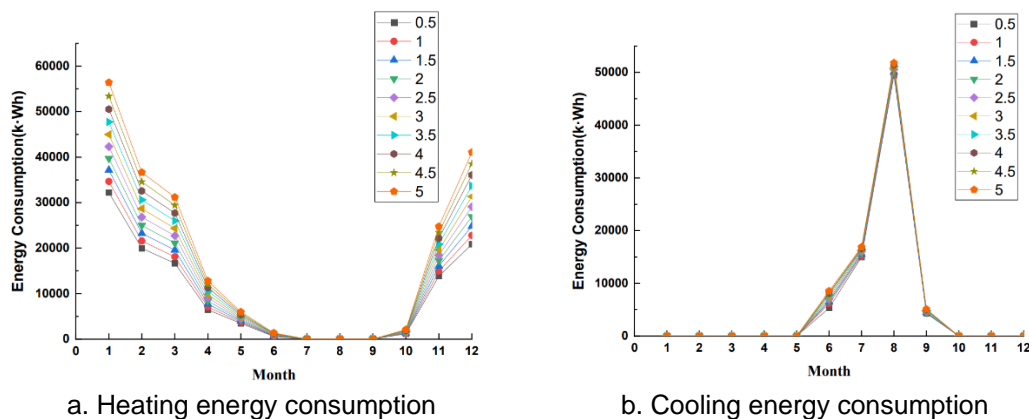

a. Heating energy consumption   b. Cooling energy consumption

Fig. 17. Influence of airtightness on building energy consumption

Impact of building structure type on building energy consumption

The annual energy consumption of the above three structure types is shown in Fig. 18. For changing only the building structure type, the annual energy consumption of the building does not change much and is still mainly influenced by the heat transfer coefficient of the envelope. However, compared to buildings with CLT and concrete structures, the walls and floor slabs of the glued laminated timber light-wood frame construction shear wall system are thinner, which has less impact on the interior space dimensions and greater space utilization. However, concrete structures are mostly cast on site, and the building integrity is better than that of timber structures after maintenance according to code

requirements. The average number of air changes in two different concrete buildings tested by Kyung-Hwan Ji *et al.* (2021) was 1.71 h^{-1} and 3.80 h^{-1}, respectively, which were both smaller than the results measured in this paper. Additionally, the air permeability q_{a50} under the reference pressure difference (50 Pa) can be calculated by Eq. 5 (Dong *et al.* 2019), where n_{50} is the number of air changes, q_{50} is the air leakage from the floor or envelope, V is the interior volume, and A is the area of the floor or envelope:

$$n_{50} = \frac{q_{50}}{V} = \frac{q_{a50} \cdot A}{V} \tag{5}$$

The energy consumption of concrete buildings is approximately 8 to 10 GJ/m^2, while the energy consumption of wood-frame buildings is only 3 GJ/m^2 (Dong *et al.* 2019). Therefore, although the airtightness of concrete buildings will be better than that of wood-frame buildings, it is clear from the discussion earlier that the lower number of air changes during the use of the building may lead to an increase in some of the operational energy consumption, and thus the energy consumption of concrete buildings will be higher than that of wood-frame buildings during the operational phase of the actual use of the building.
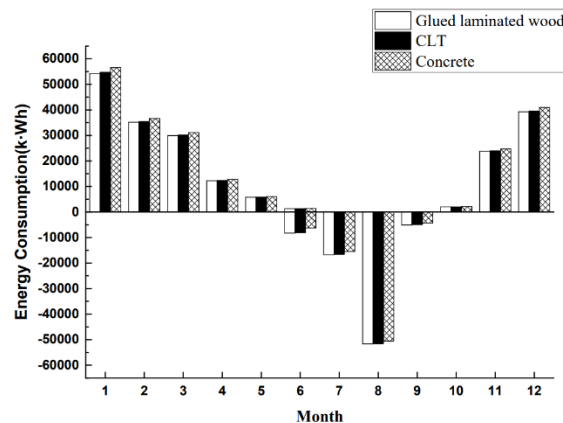

Fig. 18. Energy consumption diagram of three structural types of buildings

Impact of window-to-wall ratio on building energy consumption

Except for the stairwell, the windows on the facade have been reduced to 0.8 times their original size to investigate the effect of the window-to-wall ratio on the energy consumption of the building. After modifying the model, the window-to-wall ratio of the R&D center building was reduced from 0.32 to 0.20. A histogram of month-by-month energy consumption with reduced window-to-wall ratios is shown in Fig. 19, the overall heat gain and loss of the building is shown in Fig. 20.
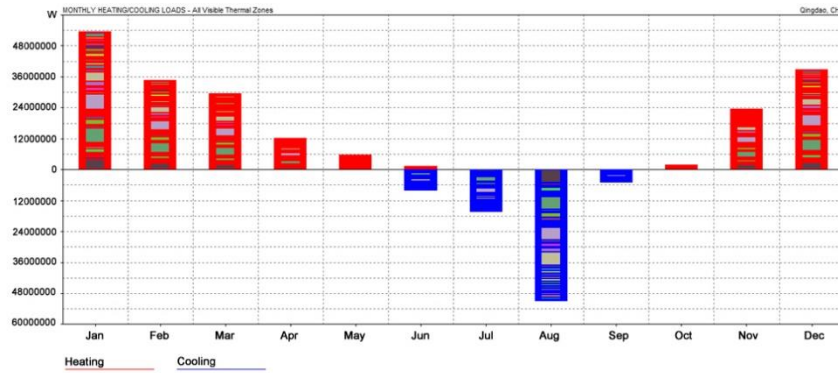
Fig. 19. Histogram of annual cooling and heating energy consumption of R&D center (window to wall ratio is reduced)
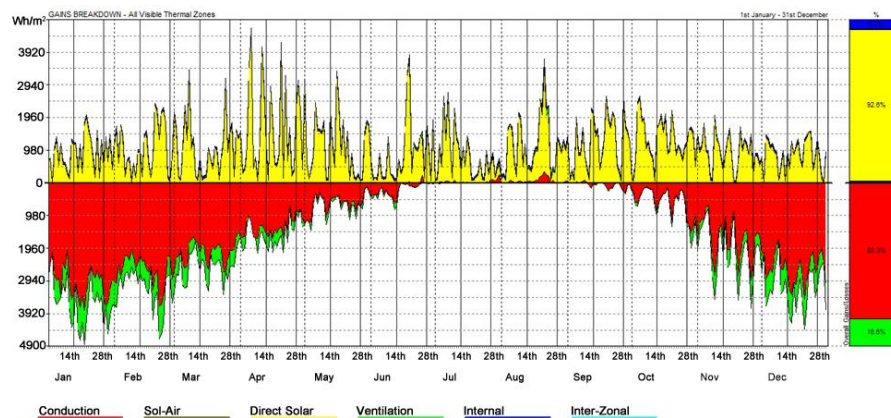
Fig. 20. The annual heat gain and loss curve of the R&D center building (window-to-wall ratio is reduced)

After the window-to-wall ratio of the R&D center building is reduced, the trend of its cooling and heating energy consumption does not change significantly with the annual heat gain and loss. The total annual energy consumption compared to the window wall was 3238 kW·h lower than before the change, accounting for about 1.1% of the total before the change, and the reduction of heating energy consumption was greater than that of cooling energy consumption. There is a certain reduction in both heat gain and heat loss for the whole year, but the proportion of each part was basically unchanged. According to "General Specification for Energy Conservation and Renewable Energy Use in Buildings" the maximum design value of window heat transfer coefficient was 2 W/m^2·K. With K$_{window}$ = 2 W/m^2·K, further calculation by Eq. 4 shows that the comprehensive heat transfer coefficient of exterior wall was 0.91 W/m^2·K at this time. When the window-wall ratio is reduced to 0.2, the comprehensive heat transfer coefficient of exterior wall was reduced to 0.72 W/m^2·K, and the difference was 0.13 W/m^2·K. The heat transfer coefficient of the windows used in this building was less than 2 W/m^2·K, so the difference of the integrated heat transfer coefficient of the envelope will be further reduced before and after the change of the window-to-wall ratio. Therefore, only adjusting the window-to-wall ratio of the building was not sufficient to effectively reduce the energy consumption of the building.

It can be seen that the window-to-wall ratio had no significant effect on the annual heating and cooling energy consumption of the R&D center building, probably because the building is located in a cold region, where the solar radiation is weak for a long time, and the change of window area has a low impact on the indoor temperature. Therefore, under the condition of meeting the design requirements, the window opening position and window opening area should be reasonably arranged to meet the demand of indoor ventilation and lighting.

CONCLUSIONS

1. The annual energy consumption per unit area for heating and cooling of the existing building was 62.7 kW·h, which is in line with the current energy consumption of small and medium-sized office buildings. The energy consumption for cooling was mainly concentrated in summer, and the energy consumption for heating was mainly concentrated in winter and early spring, with the largest energy consumption for heating in January and the largest energy consumption for cooling in August. The heat gained by the building due to solar radiation throughout the year accounted for the majority of 93.6%, and the heat loss is mainly due to heat transfer to the outside in the form of heat conduction through the envelope or heat loss due to air leakage, which accounted for 82.5% and 14.7%, respectively.

2. Airtight performance has a significant impact on building energy consumption. For example, in Shandong, the number of air changes has a much greater impact on heating energy consumption than cooling energy consumption. Further, when the airtightness is low, indoor heat is not easily dissipated to the outside in summer, which will cause the energy consumption for cooling to increase. However, from an overall perspective, reducing the number of air changes in buildings in cold regions can reduce building energy consumption. In that case, air circulation ratio should be kept within a reasonable range to avoid a significant increase in cooling energy consumption due to the inability to transfer heat to the outside in summer.

3. Under the same conditions, the building structure type and window-to-wall ratio have almost no effect on the energy consumption of the R&D center building. However, compared with the glued laminated timber beam-column frame and light wood-frame shear wall structures, the walls and floor slabs of CLT and concrete structures are thicker, which has a greater impact on the interior space dimensions. Moreover, concrete buildings are assembled with integral pouring. For that reason, the integrity is better than timber structures, and the airtightness is lower than timber structures. Thus, the energy consumption of concrete structure buildings in the use phase are lower than timber structures.

Prospect

Energy consumption simulation and analysis is an important means to assess the energy consumption and performance of glued laminated timber frame buildings, which is important for realizing building energy efficiency and environmental protection. This study provides a reference for the research on glued laminated timber frame buildings in terms of energy consumption and promotes the development and application of g glued laminated timber frame buildings. In the future, glued laminated timber frame buildings can achieve

efficient use and saving of building energy by integrating and optimizing the building energy system, so as to achieve sustainable development and environmental protection goals.

ACKNOWLEDGMENTS

REFERENCES CITED

Alfano, F. R. D., Dell'Isola, M., Ficco, G., and Tassini, F. (2012). "Experimental analysis of air tightness in Mediterranean buildings using the fan pressurization method," *Building and Environment* 53(5), 16-25. DOI: 10.1016/j.buildenv.2011.12.017.

Ambrose, M., and Syme, M. (2017). "Air tightness of new Australian residential buildings," *Procedia Engineering* 180, 33-40. DOI: 10.1016/j.proeng.2017.04.162

Cao, X. Y., Yu, W., Xiong, J., Du, C. Q., Li, N., and Yao, R.M. (2022). "Energy saving technology scheme for residential buildings in hot summer and cold winter areas based on energy consumption limits," *Heating, Ventilation and Air Conditioning* 52(07), 41-52. DOI: 10.19991/j.hvac1971.2022.07.05

Dong, H., and Li, Y. J. (2018). "Calculation of average heat transfer coefficient of light wood structure building envelope," *Construction Technology* 355(05), 16-19. DOI: 10.16116/j.cnki.jskj.2018.05.004

Dong, Y., Cui, X., Yin, X., Chen, Y., and Guo, H. (2019). "Assessment of energy saving potential by replacing conventional materials by cross laminated timber (CLT)—A case study of office buildings in China," *Applied Science-Basel* 9(05), article 858. DOI: 10.3390/app9050858

Feng, X. H., Yan, D., Peng, C., Jiang, Y. (2014). "Analysis of the impact of building airtightness on residential energy consumption," *Heating, Ventilation and Air Conditioning* 44(02), 5-14.

GB 50176-2016 (2016). "Thermal design code for civil buildings," Standardization Administration of China, Beijing, China.

GB 55015-2021 (2021). "General specification for energy conservation and renewable energy use in buildings," Standardization Administration of China, Beijing, China.

GB/T 23483-2009 (2009). "Test methods for heat transfer coefficient and heating heat supply of building envelope structure," Standardization Administration of China, Beijing, China.

GB/T 34010-2017 (2019). "Method of determining airtightness of buildings by fan pressure method," Standardization Administration of China, Beijing, China.

GB/T 34342-2017 (2017). "Standard for the test method of heat transfer coefficient of envelope structure," Standardization Administration of China, Beijing, China.

Geng, X. (2018). "Experimental discussion on the conservation and utilization of ancient Chinese wooden structures," *Heritage and Conservation Research* 3(06), 76-81. DOI: 10.19490/j.cnki.issn2096-0913.2018.06.013

Hong, G., and Kim, C. (2022). "Experimental analysis of airtightness performance in high-rise residential buildings for improved code-compliant simulations," *Energy and Buildings* 261, article ID 111980. DOI: 10.1016/j.enbuild.2022.111980

ISO 9972 (2015). "Thermal performance of buildings - Determination of air permeability of buildings - Fan pressurization method," International Organization for Standardization, Geneva, Switzerland.

JGJ/T 357-2015 (2015). "Technical procedures for field testing of heat transfer coefficient of envelope structures," Standardization Administration of China, Beijing, China.

Ji, K. H., Lee, D. S., and Jo, J. H. (2021). "A comparison of airtightness according to airtight quality construction in multi-unit residential buildings," *Collected Papers of Korea Building Environmental Protection Equipment Society* 15(3), 231-238.

Kalamees, T. (2007). "Air tightness and air leakages of new lightweight single-family detached houses in Estonia," *Building and Environment* 42(6), 2369-2377. DOI: 10.1016/j.buildenv.2006.06.001

Leonel, M., Rodolfo, L., and Li, H. T. (2022). "An innovative digital workflow to design, build and manage bamboo structures," *Sustainable Structures* 2(1), article ID 000011. DOI: 10.54113/j.sust.2022.000011

Lin, L. S., Jiang, Y., Yan, D., and Peng, D. (2015). "Analysis of broad construction energy consumption and CO_2 emissions in China's construction industry," *China Energy* 37(03), 5-10.

Lin, Z. H., and Song, Y. H. (2022). "Optimized design of air tightness of slab joints for near-zero-energy lightweight assembled buildings," *Building Energy Efficiency* 50(06), 52-58+78.

Liu, Y. Y., Li, A., Cao, J. X., and Yu, D. (2022). "Mechanical properties of timber-concrete connections with steel tube connectors," *Sustainable Structures* 2(2), article ID 000017.

Ma, Y. X., and Cong, Y. (2020). "Impact of meteorological factors on high-rise office building energy consumption in Hong Kong: From a spatiotemporal perspective," *Energy & Buildings* 228(3), article ID 110468. DOI: 10.1016/j.enbuild.2020.110468

Pan, W. (2010). "Relationships between air-tightness and its influencing factors of post-2006 new-build dwellings in the UK," *Building and Environment* 45(11), 2387-2399. DOI: 10.1016/j.buildenv.2010.04.011

Peng, Y. B., Wang, Z. H., and Ai, X. Q. (2018). "Wind-induced fragility assessment of urban trees with structural uncertainties," *Wind & Structures* 26(1), 45-56. DOI: 10.12989/was.2018.26.1.045

Šadauskienė, J., Šeduikytė, L., and Paukštys V., Banionis, K., and Gailius, A. (2016). "The role of air tightness in assessment of building energy performance: Case study of Lithuania," *Energy for Sustainable Development* 32, 31-39. DOI: 10.1016/j.esd.2016.02.006

Sfakianaki, A., Pavlou, K., Santamouris, M., Livada, I., Assimakopoulos, M. N., Mantas, P., and Christakopoulos, A. (2008). "Air tightness measurements of residential houses in Athens, Greece," *Building and Environment* 43(4), 398-405. DOI: 10.1016/j.buildenv.2007.01.006

Wang, Z. H., Wang, Z., Wang, B. J., Wang, Y., Liu, B., Rao, X., Wei, P., and Yang, Y. (2014). "Dynamic testing and evaluation of modulus of elasticity (MOE) of SPF dimension lumber," *BioResources* 9(3), 3869-3882. DOI: 10.15376/biores.9.3.3869-3882

Wang, Z. H., Gao, Z. Z., Wang, Y. L., Cao, Y., Wang, G. G., Liu, B., and Wang, Z. (2015). "A new dynamic testing method for elastic, shear modulus and Poisson's ratio of concrete," *Construction and Building Materials* 100, 129-135. DOI: 10.1016/j.conbuildmat.2015.09.060

Wang, Z. H., Wang, Y. L., Cao, Y., and Wang, Z. (2016). "Measurement of shear modulus of materials based on the torsional mode of cantilever plate," *Construction and Building Materials* 124, 1059-1071. DOI: 10.1016/j.conbuildmat.2016.08.104

Wang, Z., Xie, W. B., Wang, Z. H., and Cao, Y. (2018). "Strain method for synchronous dynamic measurement of elastic, shear modulus and Poisson's ratio of wood and wood composites," *Construction & Building Materials* 182, 608-619. DOI: 10.1016/j.conbuildmat.2018.06.139

Wang, Z., Xie, W. B., Lu, Y., Li, H.T., Wang, Z.H., and Li, Z. (2019). "Dynamic and static testing methods for shear modulus of oriented strand board," *Construction and Building Materials* 216, 542-551. DOI: 10.1016/j.conbuildmat.2019.05.004

Wang, Z. H., and Roger, G. (2021). "An extended polynomial chaos expansion for PDF characterization and variation with aleatory and epistemic uncertainties," *Computer Methods in Applied Mechanics and Engineering* 382, article ID 113854. DOI: 10.1016/j.cma.2021.113854

Wang, Z. H., and Roger, G. (2022). "A functional global sensitivity measure and efficient reliability sensitivity analysis with respect to statistical parameters," *Computer Methods in Applied Mechanics and Engineering* 402(SI), article ID 115175. DOI: 10.1016/j.cma.2022.115175

Xiong, J., Liu, Y., Li, B. Z., and Yao, R.M. (2022). "Current status of airtightness of residential buildings in Yangtze River basin and its control needs during the heating and cooling period," *Heating, Ventilation and Air Conditioning* 52(10), 1-11. DOI: 10.19991/j.hvac1971.2022.10.15

Zhang, D. Y., Gong, M., Zhang, S. J., and Zhu, X. D. (2022a). "A review of tiny houses in North America: Market demand," *Sustainable Structures* 2(1), article ID 000012. DOI: 10.54113/j.sust.2022.000012

Zhang, L., Yang, X. J., Chen, Z. H., Dong, H. R., Tan, Y. J., and Bai, X. C. (2022b). "Properties and durability of wood impregnated with high melting point polyethylene wax for outdoor use," *Journal of Wood Chemistry and Technology* 42(5), 342-351. DOI: 10.1080/02773813.2022.2095404

Zhang, X. D., Gong, T. R., Guo, Q., and Liu, Y.L. (2016). "Study on the effect of air tightness on residential energy consumption," *Building Energy Efficiency* 44(04), 61-64.

Zuo, W. C., and Wang, W. (2017). "Research on the repair and protection strategy of ancient wooden buildings - taking Yingxian wooden pagoda as an example," *Residential Science and Technology* 37(06), 19-21. DOI: 10.13626/j.cnki.hs.2017.06.004